



ACOUSTICS 2012

Scattering of complex geometries by Finite Element Method

N. González-Salido^a, A. Islas-Cital^b, F. Camarena^a, R. Pico^a and P.R. Atkins^b

^aUniversidad Politecnica de Valencia, Paranimf 1, 46730 Gandia, Valencia, Spain, 46730 Gandia, Spain

^bUniversity of Birmingham, School of Electronic, Electrical & Computer Engineering, Gisbert Kapp Building, University of Birmingham, Edgbaston, B15 2TT Birmingham, UK
rpico@fis.upv.es

The back-scattering of plane waves by complex targets of finite geometry is investigated. The information obtained from the echoes (in amplitude and phase) is used to characterize properties of the scatterers including shape, size and orientation. Simple geometries including spheres, cylinders and spheroids are often used in underwater acoustic and medical imaging to model the scattering of structures, such as fish swim bladders, blood cells, or heart fibers. Theoretical models include the effects of diffraction, reflection and transmission linked to shape, composition and size relative to the wavelength of the different objects. In particular, analytical solutions derived by Faran exist for simple geometries such as spheres and cylinders, but for more complex cases, numerical methods such as the T-matrix, or approximate simple solutions must be used. In this work, the Finite Element Method (FEM) was used to model the scattering from submerged targets with simple geometries with elastic and rigid boundary conditions. A vibroacoustic model is used to couple the structure with the surrounding fluid medium. Numerical results show good agreement with analytical solutions and experimental data.

1 Introduction

The acoustic scattering of a body contains relevant information about the properties of the target, including material composition, size and orientation. Exploring and understanding the underlying mechanisms of the formation of the echo, is necessary in order to develop reliable methods for the automatic identification of the target. One of the most important theoretical frameworks for this problem is the Resonant Scattering Theory (RST) [1]. It has shown that, for elastic targets, the fluctuating frequency domain behaviour of the scattered signal is caused by the superposition of modal resonances on the scattering response of a perfectly rigid body. Between two resonance frequencies, the scattering shows behaviour similar to that of an impenetrable rigid body. These elastic effects often play a dominant role in the overall scattering response, particularly at the intermediate frequency ranges, where the wavelength is comparable to the target dimensions. This frequency range is particularly important for fisheries acoustics.

In general, the interacting effects of unknown target orientation and composition present one of the most serious challenges for acoustic data interpretation [2]. Target strength (TS) alone has proven insufficient to discriminate between similar acoustics echoes, since widely dissimilar targets can present the same TS under differing conditions. In this context, target phase has been explored as an additional source of information for acoustic target identification. The phase of the echo is usually ignored in conventional studies, however, it has been shown [3] that the characteristics of the phase of a signal reflected from an object manifest many of its material properties, so the study of the complex scattering from fundamental finite shapes, such as spheres and cylinders can provide key insights into the mechanisms of echo formation and the connection between phase and target characteristics.

In the present paper, the problem of sound scattering of a plane wave, normal and obliquely incident on an elastic cylinder of finite length and a prolate spheroid submerged in water is considered. The work presented here provides a direct comparison of experimental measurements presented in [4], and numerical results obtained by using the Finite Element Method with a vibroacoustic model that couples the target structure with the surrounding fluid medium.

2 Finite element modeling

A finite element simulation of rigid and elastic target was obtained using the commercial FE software COMSOL Multiphysics. Two different models have been chosen to simulate the scattering of a plane wave by finite length

targets. For axially incident waves, the axial symmetry of the target (sphere, finite cylinder and prolate spheroid) warrants the use of 2D-aximetric models, with a significant resolution of computational cost. For other angles of incidence 3D models are used, as illustrated in Figure 1. The mirror symmetry of the xy plane is taken into account for simulations. Both models consist of an elastic or rigid body of finite length submerged in a fluid domain of water bounded by a perfect matched layer (PML). The PML has a width of 2 cm meshed with a 6.8 mm element size. In Table 1 the parameters of each simulation are presented, including size, Young's modulus, Poisson's ratio, density, and the number of elements for the minimum wavelength simulated in both media.

Table 1: Targets parameters used for numerical simulations.

	Tungsten carbide sphere	Steel cylinder	Aluminium spheroid
Radius (cm)	4.2	1	1.5
Length (cm)		12	12
Young's modulus (MPa)	614.5	190.7	70
Density (Kg/m ³)	15022	7910	2700
Poisson's ratio	0.202	0.254	0.33
Elements (Target/Water)	10/8	8/6	8/6

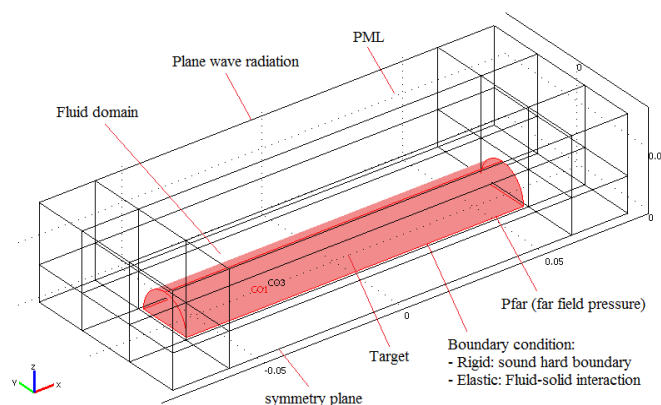


Figure 1: Schema of the FE model.

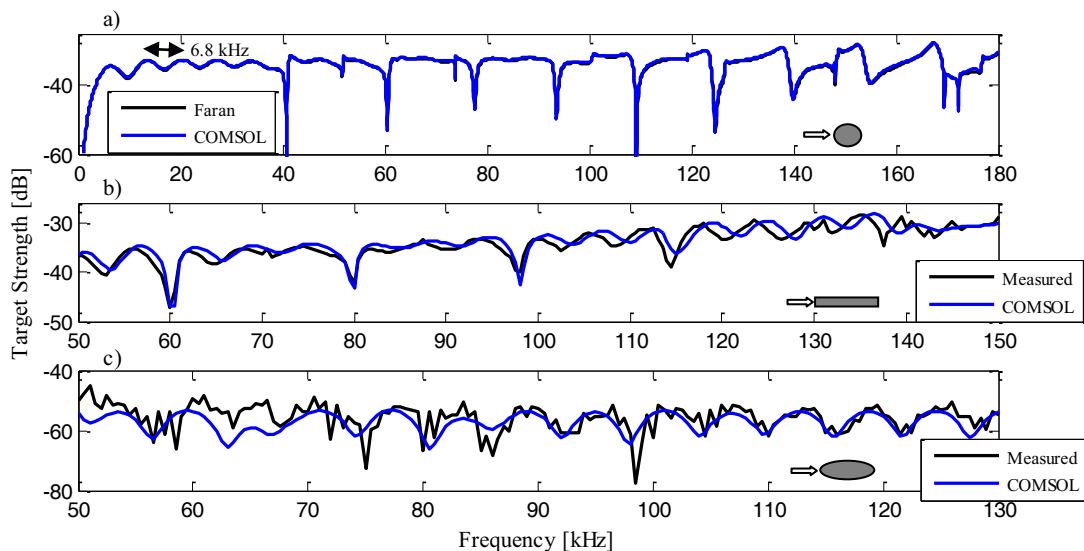


Figure 2: Target Strength from a: a) Tungsten carbide sphere, b) steel cylinder in end-on incidence, c) Aluminium prolate spheroid in end on incidence. The associated target dimensions are provided in Table 1.

3 Amplitude and phase scattering in end-on incidence

The results for both amplitude and phase of the scattered pressure by different targets are presented in this section. A 2D-axisymmetric model is used and the incident plane wave is considered to propagate along the axial direction.

3.1 Target Strength

In Figure 2 the TS of a tungsten carbide sphere, a steel finite cylinder and an aluminium prolate spheroid are presented. The TS of the tungsten carbide sphere, shown in Figure 2.a is compared with the Faran analytical model [5], with differences smaller than 0.5 dB between both models across the entire frequency range. Resonances associated with the maxima (and minima) of the TS and correspond to specific eigenmodes excited by different circumferential waves that encircle the target and interact constructively and destructively. Therefore, the resonances are related to the dimensions and composition of the object. For the case of elongated bodies, resonances may occur due to waves propagating in meridional and helical paths and reflected from the far end [6].

Figures 1.b and 1.c show the TS from the cylinder and

spheroid respectively, compared with measured data

The RMS difference across the entire bandwidth between experimental data and the models is approximately 1.6 dB for the cylinder. In the case of the prolate spheroid, the broadband RMS error is higher, close to 5dB, although the general trend of the response indicates modest agreement. The sources of error can largely be ascribed to experimental factors, such as a lack of exact knowledge about material composition, and inaccuracies in the target rotation mechanism.

3.2 Target Phase

The phase information can be extracted, as in the case of amplitude, from the acoustic response following the procedure detailed in [7], using a differential phase measurement between two excitation frequencies, with the aim of removing range effects.

Figure 3 illustrates the target phase of a sphere, cylinder and spheroid at end on incidence. The validation is performed by comparing the numerical results, with modal solutions [5] in the case of the sphere, and measured data in the other cases. In Figure 3.a, the numerical results are shown to be very accurate in comparison to the theoretical model. Agreement is also found between measured and model data for the cylinder in Figure 3.b and the spheroid in Figure 3.c.

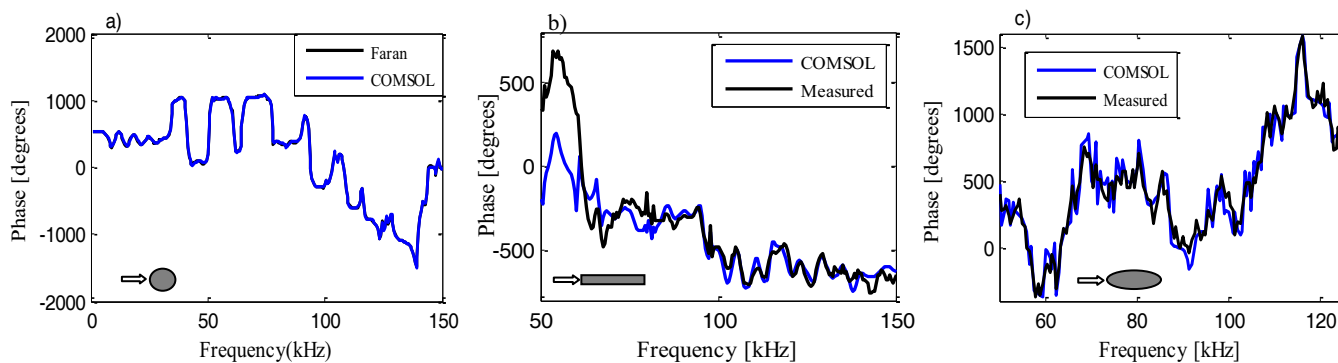


Figure 3: Target phase from a: a) Tungsten carbide sphere, b) steel cylinder and c) Aluminium spheroid in end-on incidence obtained using a dual frequency transmission method.

The analysis of target phase, and in particular differential target phase is complicated by random 2π ambiguities and artefacts associated with the unwrapping process. This can be observed in the case of cylinder, where the low frequency features agree more closely after 2π factors are removed. For the prolate spheroid in Figure 3.c these ambiguities have been eliminated, but the correction algorithm results in a somewhat ragged appearance.

The phase response is related to the geometry and material composition of the target. In the case of a solid sphere, Figure 3.a, a smooth oscillatory regime is present at low frequencies, between 0 and 30 kHz. This behaviour is similar to the oscillation observed in Figure 2.a in the amplitude curve. Both are due to the interference pattern created by diffraction of surface Franz waves. Their period

frequency, f_{Franz} , is given by the path length; it can be obtained from the following expression [8]

$$f_{\text{Franz}} = \frac{1.22c}{2\pi a} \quad (1)$$

which for a speed of sound $c=1486$ m/s, and a sphere with radius $a = 84$ mm, is approximately equal to 6870 Hz, which corresponds to the period observed in Figure 2.a and 3.a.

In the resonant regime, important phase changes with respect to frequency are present, and may be related to the coupling angles of longitudinal, shear, or Rayleigh waves.

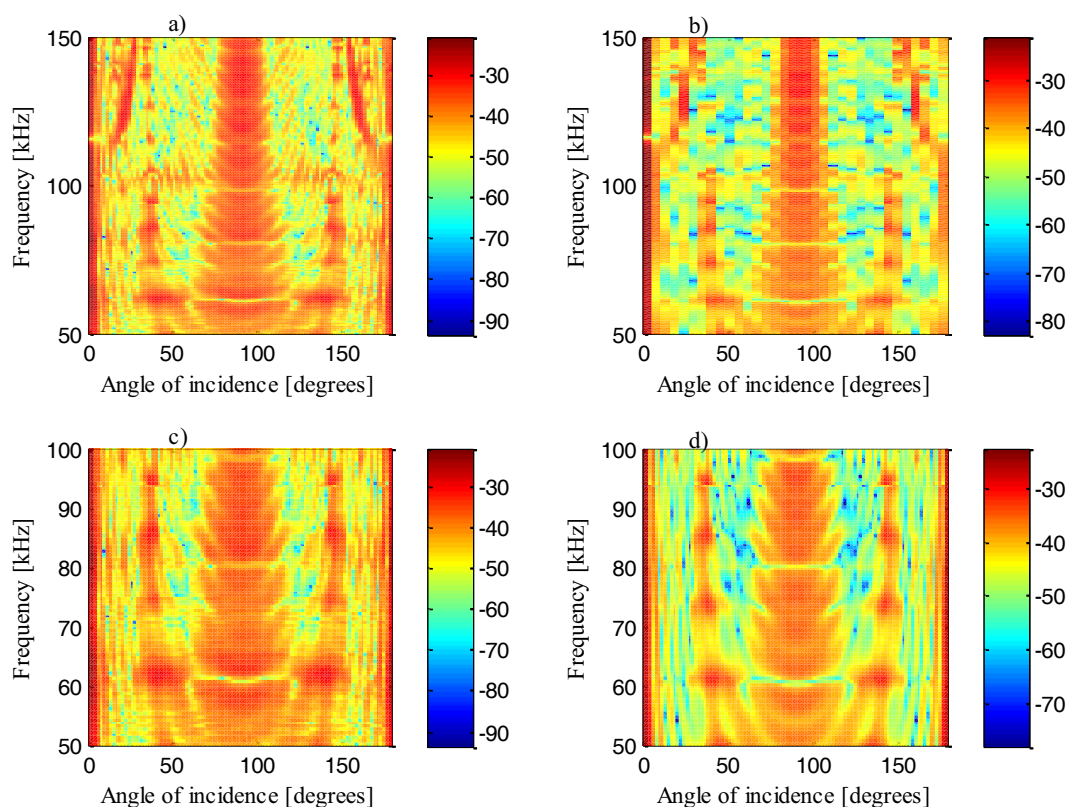


Figure 4: TS from 12 cm-long steel cylinder as a function of orientation and frequency. a) and c) illustrate measured data with a frequency step of 500 Hz and angle step of 1.8. b) and d) illustrate the numerical results obtained with a frequency step of 500 Hz and angle step of 5.4° in b) and 1.8° in d).

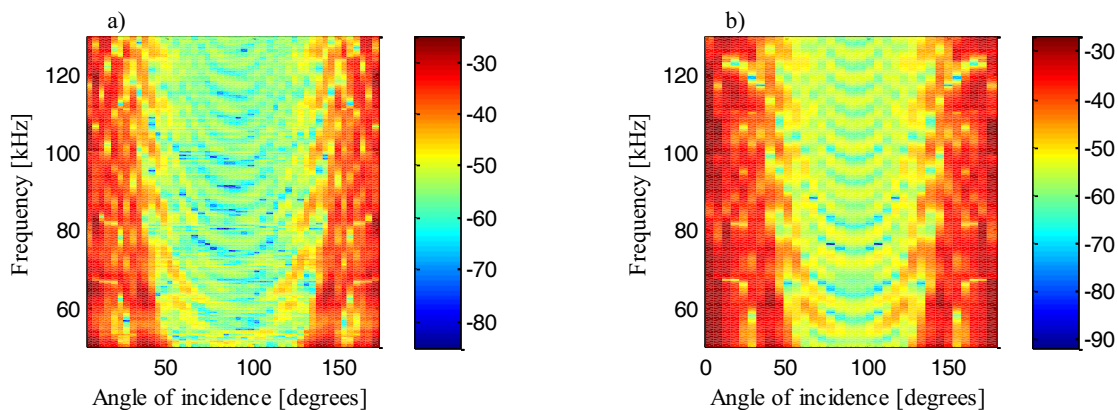


Figure 5: TS from 12 cm-long aluminium prolate spheroid as a function of orientation and frequency. a) illustrates the experimental measurements with a frequency step of 500 Hz and angle step of 1.8, and b) illustrates numerical results with a frequency step of 500 Hz and angle step of 5.4°.

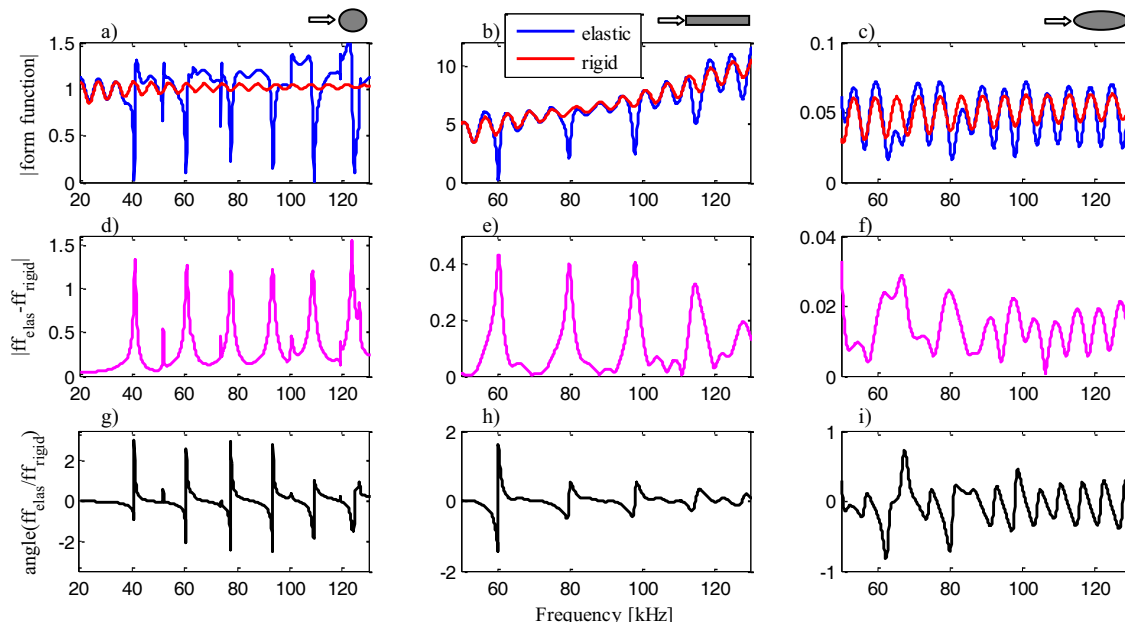


Figure 6: Rigid and elastic form function (a,b,c), resonant spectrum (d,e,f) and phase spectrum (g,h,i) for a tungsten carbide sphere (a,d,g), steel cylinder (b,e,h) and aluminium spheroid (c,f,i) in end on incidence.

4 Target strength an obliquely incidence

Finite cylinders and spheroids are useful for the study of the effects of oblique incidence on an elongated body. Analytical models in this case are not simple or not available for specific geometries. Thus, experimental measurements have been analyzed by comparison with the simulation results provide by numerical methods such as FEM.

FEM and measured target strength results for the steel cylinder are presented in Figure 4 where 0° and 180° correspond to broadside incidence and 90° is end-on incidence. All figures show results obtained with a 500 Hz frequency step. The angular resolution is 1.8° in the experimental measurements and 5.4° for the numerical simulations presented in Figure 4.b and 1.8° in Figure 4.d. It is evident that better agreement occurs between Figures 4.c and 4.d. Due to the computational costs of the fine mesh at high frequencies, the frequency range covers from 50 kHz to 100 kHz.

Figure 5 illustrates FEM and measured target strength results for the aluminium spheroid with a 500 Hz frequency step and a rotation resolution of 3.6° for the measured data, Figure 5.a, and 5.4° for the COMSOL data, Figure 5.b. The agreement in this case is better than that for the cylinder, despite the poor angular resolution. The TS is strongly influenced by the geometry and orientation of the target. Agreement improves near end on incidence, where the cylinder has brighter specular features due to the flat end caps.

5 Resonant and Phase spectrum

One of the advantages of FEM in the study of the scattering of an elastic object is that it can obtain the rigid scattering response for the same geometries. According to resonant scattering theory [1], the scattering response of a hard elastic object is comprised a series of superimposed

resonances in a background rigid response. Thus, it is possible to obtain the resonant spectrum from the difference between the elastic and rigid responses. In Eq. (2), ff indicates the normalized amplitude pressure or form function.

$$RS = \left| ff_{elastic} - ff_{rigid} \right| \quad (2)$$

In this work, we investigate the information that can be extracted from the phase. With this goal, a phase spectrum (PS) is defined from the angle of the ratio of elastic and rigid form functions, as defined in Eq. (3). With this formulation, the phase does not include the information concerning the measurement range, and only provides the phase counterpart related to the elastic properties of the target.

$$PS = angle \left(\frac{ff_{elastic}}{ff_{rigid}} \right) \quad (3)$$

5.1 End on incidence

Figure 6 illustrates the elastic and rigid form functions (first row), and the resonant and phase spectrum (second and third row) for the three simulated targets in end-on incidence.

In the first two cases, the sphere and cylinder, each form function of the elastic target shows a rigid behaviour followed by the excitation of some resonances, which appear superimposed on the background rigid response.

The non-null values of the resonant spectrum are related to the excitation of the resonances. Likewise, it is noted that the phase spectrum, shown in the last row of Figure 6, is null for the frequencies and angles for which the elastic target presents a rigid behaviour, since, as expected, both rigid and elastic targets have the same form function as both amplitude and phase. In the region of resonance, Figures 6.g and 6.h exhibit phase shifts in the excitation of

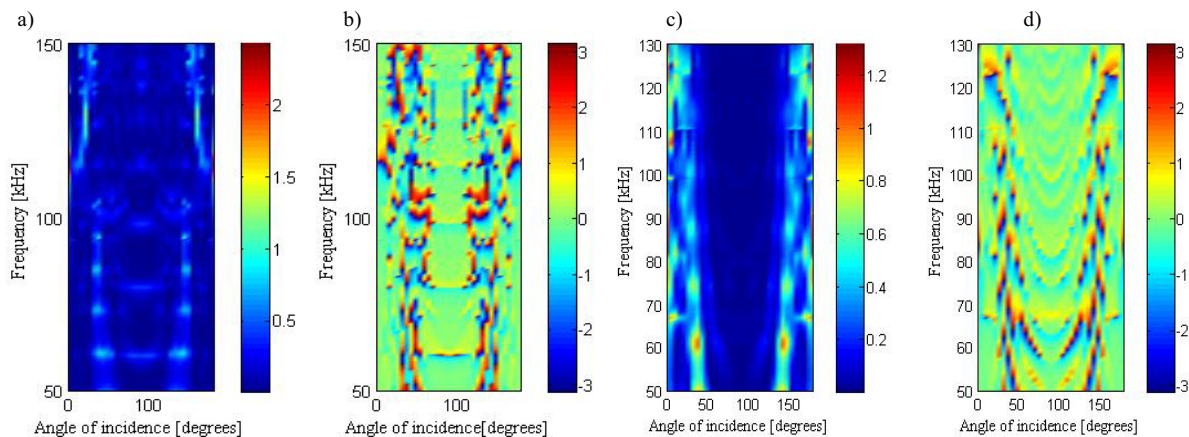


Figure 7: Resonant (a,c) and phase (b,d) spectrum for steel cylinder (a,b) and aluminium spheroid (c,d).

resonances, which can be associated with abrupt changes phases observed in the region of resonance in Figure 2.

For the spheroid, although the resonant theory is also valid [9], very close eigenmodes with small amplitude are excited, so the identification of the resonances in the resonant spectrum, which maximum is 0.03, and the phase shifts in the phase spectrum are not obvious.

5.2 Obliquely incidence

Finally, Figure 7 shows the resonant spectrum (7.a, 7.c), and the phase spectrum (7.b, 7.d), for the steel cylinder (7.a, 7.b), and aluminium spheroid (7.c, 7.d), for oblique incidence.

It is noted that effectively the resonances appear as relative maximum amplitude in the resonant spectrum, which is associated with a phase shift in the phase spectra. In fact, the detection of resonant regions is more evident through phase changes, because the resonant spectrum depends on the amplitude resonances which are more variable. A related usage of target phase also applied in the identification of resonances has been previously explored by Maze [10].

6 Conclusions

The finite element method allows the computation of the acoustic scattering by submerged, finite targets to be obtained into the resonance frequency range. The amplitude and phase of the scattering responses are consistent with the experimental results. These responses are dependent on the geometry and orientation of the target and have proven useful for identification and added understanding of scattering processes. Target phase could potentially be added as an additional parameter for characterization of scatterers. However more work is needed for an unambiguous interpretation of the phase response. In this respect, FEM simulations can be very useful. However the main obstacles in this approach are the enormous requirements for computing power, which slow down the development process and restrict the range of targets that are convenient for practical simulation.

Acknowledgments

The work was financially supported by Universitat Politècnica de Valencia through project PAID 06-10.

References

- [1] L. Flax, G.C. Gaunard, H. Uberall, "Theory of resonance scattering", *Physical acoustics*. London, Academic Press 191-294 (1981)
- [2] P.L.D. Roberts, J.S. Jaffe, "Multiple angle acoustic classification of zooplankton" *J. Acoust. Soc. Am.* 121(4), 2060-2070 (2007)
- [3] L.M. Deuser, D. Middleton, T.D. Plemons, et al, "On the classification of underwater acoustic signals. II. Experimental applications involving fish" *J. Acoust. Soc. Am.* 65 (2), 444-455 (1979)
- [4] A. Islas-Cital, "Amplitude and phase sonar calibration and the use of target phase for enhanced acoustic target characterization" *Thesis, College of Engineering and Physical Sciences*. The University of Birmingham (2011)
- [5] J. Faran, "Sound scattering by solid cylinders and spheres" *J. Acoust. Soc. Am.* 23 (4), 405-418 (1951)
- [6] X.L. Bao, "Echoes and helical surface waves on a finite elastic cylinder excited by sound pulses in water" *J. Acoust. Soc. Am.* 94 (3), 1461-1466 (1993)
- [7] P.R. Atkins, A. Islas-Cital, K.G. Foote, "Sonar target-phase measurement and effects of transducer matching" *J. Acoust. Soc. Am.* 123 (5), 39-49 (2008)
- [8] H. Medwin, C.S. Clay, "Fundamentals of Acoustical Oceanography" *CA: Academic Press*. San Diego (1998)
- [9] L. Flax, L.R. Dragonette, V.V. Varadan, V.K. Varadan, "Analysis and computation of the acoustic scattering by an elastic prolate spheroid obtained from the T-matrix formulation" *J. Acoust. Soc. Am.* 71(5), 1077-1082 (1982)
- [10] G. Maze, "Acoustic scattering from submerged cylinders MIIR Im/Re: Experimental and theoretical study" *J. Acoust. Soc. Am.* 89(6), 2559-2566 (1991)